

# **Final Report – D5**

## **Wind Farm Control and Layout Optimization for U.S. Offshore Wind Farms**

Prepared for:

**National Offshore Wind Research and Development Consortium**

Christine Sloan, Project Manager

Julian Fraize, Project Manager

Prepared by:

**National Renewable Energy Laboratory (NREL)**

Golden, CO 80401

Paul Fleming  
Principal Investigator

David Dunn  
NOWRDC Project Coordinator

Patrick Duffy, Christopher Bay, Matthew Churchfield

Rebecca Barthelmie, Sara Pryor

## Acronyms and Abbreviations

---

AEP	annual energy production
BOEM	Bureau of Ocean Energy Management
CC	cumulative curl
FLORIS	FLow Redirection and Induction in Steady State
GCH	Gauss curl hybrid
GW	gigawatt
IEA	International Energy Agency
LCOE	levelized cost of energy
MW	megawatt
nm	nautical mile
NREL	National Renewable Energy Laboratory
ORBIT	Offshore Renewables Balance-of-System and Installation Tool
SCADA	supervisory control and data acquisition
SOWFA	Simulator fOr Wind Farm Applications
TI	turbulence intensity
WRF	Weather Research and Forecasting

## Notice

---

This report was prepared by Paul Fleming in the course of performing work contracted for and sponsored by the National Offshore Wind Research and Consortium (NOWRDC), New York State Energy Research and Development Authority (NYSERDA), and the U.S. Department of Energy (hereafter the “Sponsors”). The opinions expressed in this report do not necessarily reflect those of the Sponsors or the State of New York, and reference to any specific product, service, process, or method does not constitute an implied or expressed recommendation or endorsement of it. Further, the Sponsors, the State of New York, and the contractor make no warranties or representations, expressed or implied, as to the fitness for particular purpose or merchantability of any product, apparatus, or service, or the usefulness, completeness, or accuracy of any processes, methods, or other information contained, described, disclosed, or referred to in this report. The Sponsors, the State of New York, and the contractor make no representation that the use of any product, apparatus, process, method, or other information will not infringe privately owned rights and will assume no liability for any loss, injury, or damage resulting from, or occurring in connection with, the use of information contained, described, disclosed, or referred to in this report.

NYSERDA makes every effort to provide accurate information about copyright owners and related matters in the reports we publish. Contractors are responsible for determining and satisfying copyright or other use restrictions regarding the content of reports that they write, in compliance with NYSEDA’s policies and federal law. If you are the copyright owner and believe a NYSEDA report has not properly attributed your work to you or has used it without permission, please email [print@nyserda.ny.gov](mailto:print@nyserda.ny.gov)

Information contained in this document, such as web page addresses, are current at the time of publication.

# Table of Contents

---

<b>1. Introduction</b>	<b>5</b>
<b>2. Engineering Model Calibration</b>	<b>8</b>
2.1 Modeling U.S. Offshore Locations	8
2.2 Calibration to Offshore SCADA Data	11
2.3 Calibration to High-Fidelity Computer Simulations	12
<b>3. Optimization Studies</b>	<b>14</b>
3.1 Layout Optimization	14
3.2 Wind Farm Control Optimization	18
3.2.1 Considerations on Wind Farm Control Results	20
3.3 Discussion of Optimization Results	20
<b>4. LCOE and Revenue Analysis</b>	<b>23</b>
4.1 Revenue Analysis	23
<b>5. Conclusions</b>	<b>25</b>

# 1. Introduction

---

U.S. offshore wind energy is expected to grow rapidly in the coming years with a national goal of 30 gigawatts (GW) by 2030 (The White House 2021; Musial et al. 2022). Wake losses are expected to be significant in U.S. offshore locations where low-turbulent conditions are prevalent (Bodini, 2019). For the original U.S. East Coast lease areas (excluding the 2022 additions in New York Bight), modeling with the Weather Research and Forecasting (WRF) model calculated total wake losses of more than one-third of annual electricity production (AEP) with wakes extending more than 90 km (Pryor, Barthelmie, and Shepherd 2021). In a more recent study (Rosencrans et al. in review), internal wake losses (wake losses within a wind farm, not caused by the wake of other wind farms) for a U.S. offshore wind farm in the mid-Atlantic were modeled to reduce annual power production by 27.4%.

Wind farm control is technology that coordinates the control activities of individual wind turbines within a wind farm to maximize farm-level performance, often by reducing wake losses. One implementation of wind farm control is wake steering (Wagenaar, Machielse, and Schepers 2012). Illustrated in Figure 1, wake steering uses an offset of the yaw position of the turbine with respect to the incoming wind direction to deflect and change a turbine’s wake to benefit downstream turbines.

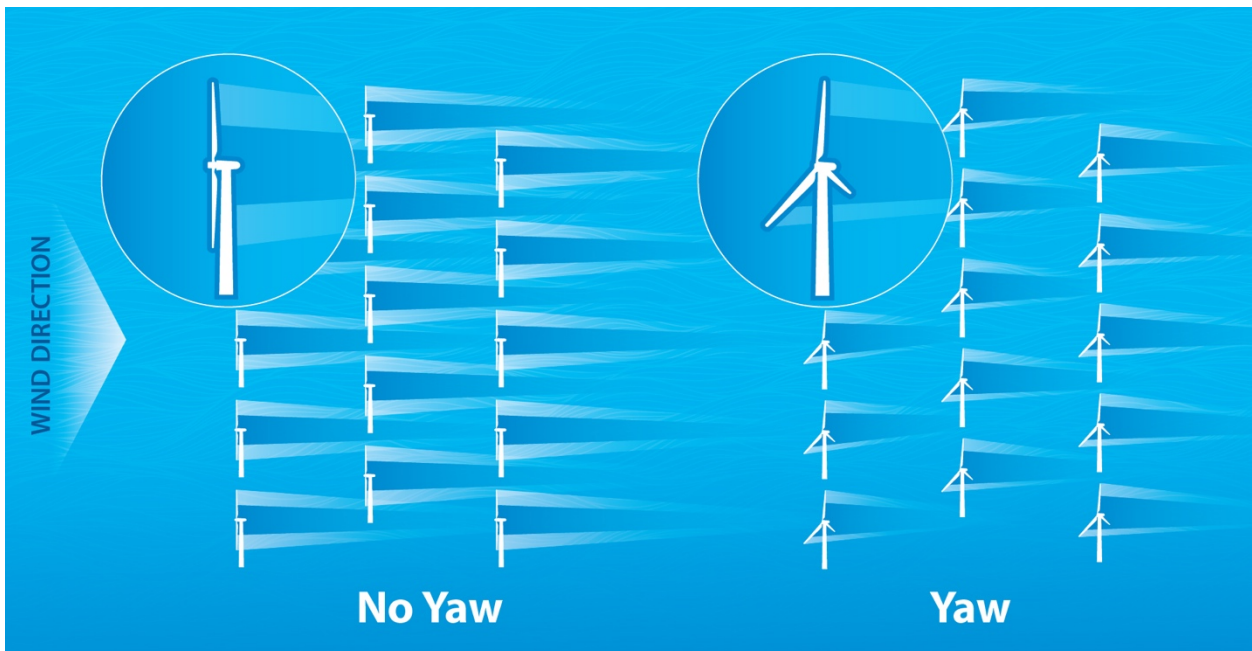


**Figure 1. Illustration of wake steering at an offshore wind farm. On the left, an array of wind turbines is aligned to the incoming wind direction, with wakes impinging on downstream turbines. On the right, the same array applies wake steering such that the wakes are modified to reduce wake losses downstream.**

Previous studies of wind farm control for land-based wind farms demonstrated the effectiveness of the technology. For example, field campaigns such as Fleming et al. (2020) and Simley et al. (2021) have shown that wake steering can effectively reduce wake losses in practice, increase energy yield, and test the accuracy of the wind farm control models used in the design of wake-steering controllers. Further, Bensason et al. (2021) used the same engineering models validated in the field campaigns to assess the potential across U.S. land-based wind farms and found a typical potential to reduce wake losses by 13.85%, increasing expected AEP by 0.8%.

Previous studies have mostly been applied to already built commercial wind farms; however, it is likely there is greater potential benefit for offshore wind farms. First, the high expected wake losses presented in Rosencrans et al. (in review) illustrate a larger opportunity for energy uplift in offshore farms versus land-based farms. Second, when applied to already existing farms, wake loss reduction strategies can only mitigate the already set annual wake losses. However, when incorporated into the design of a new wind farm, wind farm control can be used in the overall optimization of value to maximum benefit.

The purpose of this project is to investigate how wind farm controls and layout optimization can be used to benefit U.S. offshore wind farms. Note that this work focuses on fixed-bottom offshore turbines and does not consider issues specific to floating turbines, such as drift in position or wake impacts of floating motion. A partnering project, CONFLOWS, looks at these topics with respect to floating offshore wind farms (Slater 2021).

We consider both increases in AEP and reductions in levelized cost of energy (LCOE). We also show that wind farm controls can have impacts on revenues for offshore wind farms, which exceed the impacts on AEP.

The project was divided into three main phases. The first was establishing engineering models of wind turbine wakes and wind farm control that are calibrated for U.S. offshore wind farms. The second was using these calibrated models in optimizations over potential layout configurations and wind farm control strategies. In the third effort, the results of the optimizations were compared with respect to energy production and LCOE and revenue.

Details on each of the tasks for this project are provided in the task reports. This final report provides an overview of those results, final summary, and interpretation of findings. We believe an essential outcome of this work is that wind farm control should be considered an important tool for increasing the total energy

production and revenue of U.S. offshore wind farms. Control will be especially valuable if wind farms are designed to maximize the energy production of a given lease area.

## 2. Engineering Model Calibration

---

To assess the potential for wind farm control and layout optimization, an engineering model of wind farms is required. In this work, we use FLOW Redirection and Induction in Steady State (FLORIS), a wakes and wake-steering model (NREL 2022). FLORIS is an open-source software framework, developed and maintained by the National Renewable Energy Laboratory (NREL), that includes both the models and optimization tools required for this work. FLORIS has been used in the design of wake-steering controllers (Fleming et al. 2020; Simley et al. 2021) and in assessing how wake steering benefits land-based wind farms (Bensason et al. 2021).

For this work, a necessary step to performing the optimization studies was to develop models of wakes and wake steering within FLORIS that were calibrated to offshore wind turbines and specifically to U.S. offshore conditions. We subdivided this work into three aspects. First, we selected three U.S. offshore locations to study and produced atmospheric models of the locations as inputs to the FLORIS engineering model. Second, we calibrated the wake models in FLORIS to existing offshore wind farms. Third, we calibrated the wake-steering models in FLORIS to high-fidelity computer simulations.

### 2.1 Modeling U.S. Offshore Locations

To select the U.S. sites to analyze, we consulted with the project's advisory board, which included members of the wind energy industry. The final selected sites are shown in Figure 2 and include a mid-Atlantic site (Vineyard Wind Lease Area, as designated by the Bureau of Ocean Energy Management [BOEM]), a Pacific site (Humboldt Call Area, as designated by BOEM), and a Hawaiian site (South Oahu Call Area, as designated by BOEM) (BOEM Undated[a, b, c]). These sites are expected to be among the first developed for wind energy in their respective regions.



**Figure 2. Map of the selected U.S. sites. The Weather Research and Forecasting model simulation domains are shown (white outline), as well as the chosen wind farm location within each domain.**

Atmospheric inputs to FLORIS for each site were provided using simulations performed with the WRF model (NCAR 2023). For the sites shown in Figure 2, we performed new WRF simulations that leveraged the same model setup currently used to produce state-of-the-art, 20-year, offshore wind resource data sets for U.S. waters (NREL 2021). One-year simulations were performed for each of the sites, with the simulation years chosen based on monthly analysis of wind speed. We selected the year between 2000 and 2020 that best represents the mean seasonal cycle of wind speeds. The domains simulated for each site are indicated by the white outlined areas in Figure 2.

In Section 2.2, we discuss calibrating the engineering model to offshore supervisory control and data acquisition (SCADA) data. These data were obtained from three offshore European Union wind farms: Anholt, Westermost Rough, and Windpark Egmond aan Zee (OWEZ) (Doekemeijer, Simley, and Fleming 2022). (At the time of this report there was no U.S. offshore wind farm SCADA data available to the authors). To compare the atmospheric conditions between the current European Union wind farms and the proposed U.S. wind farms, data equivalent to the WRF simulations were extracted for each European Union location from the New European Wind Atlas (Hahmann et al. 2020).

The Task 1 report for the project includes a detailed analysis of the results of this study comparing atmospheric conditions between the U.S. and European Union sites; however, some of the key findings for this analysis are represented in Figure 3, which shows the distributions of wind direction and turbulence intensity for each location, with the U.S. locations in the top three rows and the European Union locations in the bottom three rows.

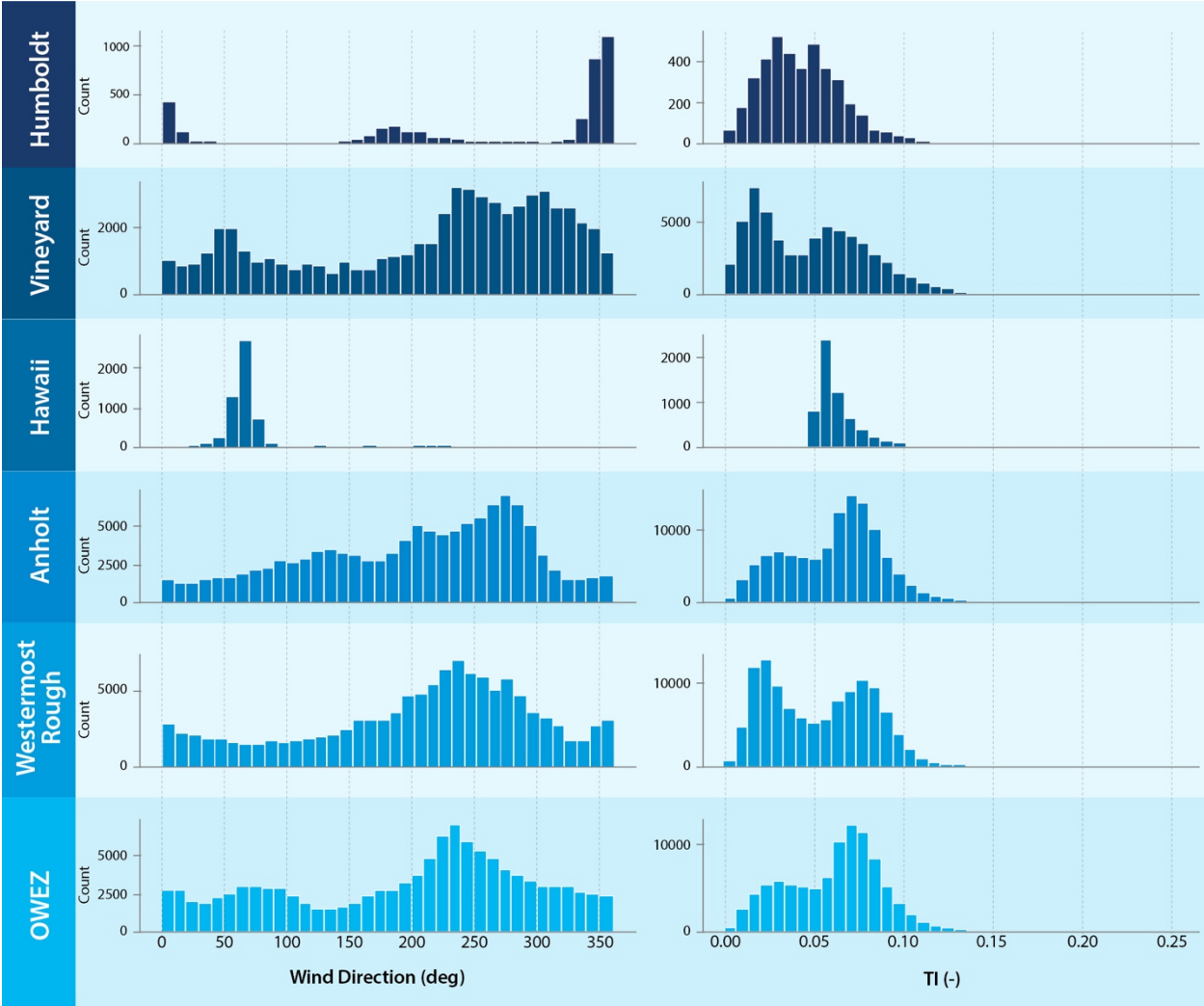


**Figure 3. Comparing the distribution of wind direction and turbulence intensity (TI) for the locations considered at turbine hub height (165 m). Note that TI is an estimate, which is approximated using turbulent kinetic energy.**

FLORIS uses frequency tables of wind speed and wind direction to compute AEP given simulations of individual wind speed and wind direction bins, whereas turbulence intensity (TI) is used by the wake

models as a factor that influences wake recovery rates; higher TI is associated with faster recovery rates and lower wake losses.

The wind direction results in Figure 3 show that while Vineyard is not too dissimilar from the European sites, both Humboldt and Hawaii show a high degree of concentration into a limited number of wind directions. This concentration will impact the layout optimization because it will provide very dominant wind directions to design to. In the case of Humboldt, the concentration of the wind rose into a dominant direction could be verified using lidar buoy data (Atmosphere to Electrons 2023).

For TI, it is important to point out that the WRF model does not directly output TI, so these values are estimated based on turbulent kinetic energy and should only be considered for their relative comparison. These distributions show that for Vineyard and Humboldt, a higher percentage of data include low, or very low, TIs versus the European locations. This outcome aligns with the findings of Bodini, Lundquist, and Kirincich (2019). Because we calibrate to European Union wind farms, there is potential that the wake losses at U.S. locations will still be higher.

## **2.2 Calibration to Offshore SCADA Data**

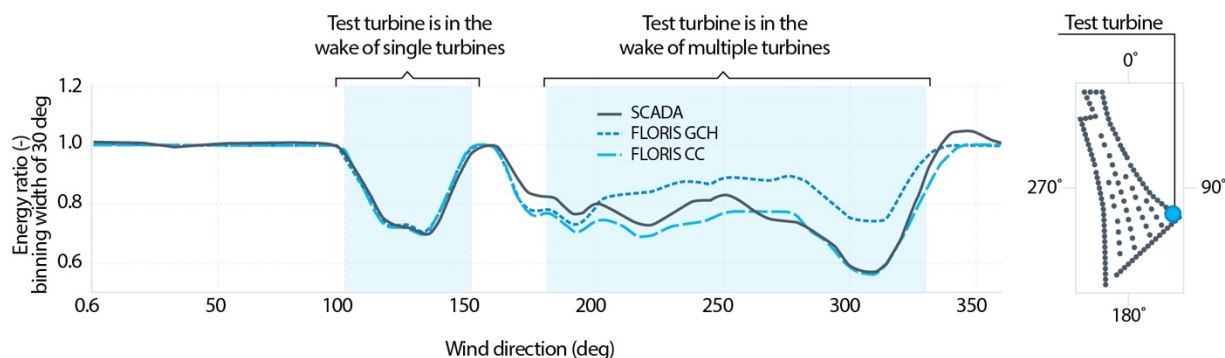
In this phase, we compared the FLORIS model of wakes to three sets of data from offshore wind energy farms. Specifically, we compared the “Gauss curl hybrid” (GCH) (King et al. 2021) model of wakes and wake steering to each of the data sets, and the results were published in Doekemeijer, Simley, and Fleming (2022).

Figure 4 represents a result observed in Doekemeijer, Simley, and Fleming (2022). In the figure, the energy ratio of a test wind turbine within the wind farm (indicated on the right) with respect to freestream unwaked wind turbines, is shown for different wind directions. For example, a value of 0.8 means that for this wind direction, the test turbine produces 80% of the energy of a freestream, or unwaked, turbine.

Focusing on the comparison between the GCH model and SCADA data, Figure 4 shows that for wind directions where the test turbine is in the wake of a single turbine, the GCH model matches well to the SCADA data. However, for directions where the test turbine is in the rear of the farm and in the wake of many upstream turbines, GCH tends to overpredict energy production. This issue—the prediction of wake losses in the rear of a large offshore wind farm array—was identified in Doekemeijer, Simley, and Fleming (2022) as the primary discrepancy between FLORIS and SCADA data. Because much of FLORIS’ tuning has been to smaller subsets of farms, either because of limitations on sizes of high-

fidelity modeling or initial field trials limited to a smaller number of turbines, the occurrence of the mismatch at the rear of large arrays makes some sense.

In Bay et al. (2022), a new model of wakes, wake combination, and wake steering, known as the cumulative curl (CC) model, is introduced. Combining a new model of wind turbine wake superposition presented in Bastankhah et al. (2021) with a near wake model from Blondel and Cathelain (2020), the model of wake steering from GCH is presented. Referring now to the plot of the prediction of energy ratios for the same test turbine in Figure 4, a much better match to wake losses in the rear of the farm is obtained. Details of the model implementations are provided in Bay et al. (2022).



**Figure 4. Comparing the energy ratios observed in SCADA data for the Anholt wind farm for a test turbine (indicated as a blue dot) in the subplot to the right) relative to freestream turbines. Note, both models are almost equal in their ability to predict the wake losses for a single wind turbine (in the range of 100–150 degrees, the turbine is waked by one turbine at a time, whereas the match to SCADA is improved significantly by the cumulative curl (CC) model in the range of 180–330 degrees, when the test turbine is in many overlapping upstream wakes. Adapted with permission from Bay et al. (2022)**

## 2.3 Calibration to High-Fidelity Computer Simulations

At the time the project was conducted, there were no SCADA data from offshore wind farms performing wake steering; as a result, the wake-steering aspects of the models were compared to new high-fidelity simulations of wind farms implementing wake steering.

The Simulator fOr Wind Farm Applications (SOWFA) was used to perform large-eddy simulations of wind farms (NREL undated). We simulated several models of gridded wind farms and generated the inflows to the wind farms to match specific periods of interest from the WRF simulations described in Section 2.1. With respect to wake deficit modeling, the SOWFA simulations agreed with the results of the SCADA analysis, with the CC and GCH models performing equally for a small number of wakes, and the CC model resolving the underprediction of wakes by the GCH model for larger numbers of combined

wakes. For wake steering, the two models are similar when modeling the effect of a single wind turbine performing wake steering. However, when assessing the uplift for a large array implementing wake steering, the SOWFA results tended to fall between the relative uplifts from the GCH (higher than SOWFA) and CC (less than SOWFA) models. These results are all provided and discussed in Bay et al. (2022).

## 3. Optimization Studies

---

Following the calibration to offshore conditions, the FLORIS model can be applied to optimization studies of layout and wind farm control. The results of these studies are presented in this section.

### 3.1 Layout Optimization

The original proposal for this project was to analyze layout optimizations against a range of potential objective functions and against a range of hypothetical boundary areas of simple shapes. However, in consultation with the project advisory board, it was decided that a more relevant optimization would take the following approach:

1. Adopt realistic boundary areas
2. Assume a minimum interturbine spacing of 1 nautical mile (nm)
3. Assume the wind turbines must be on a grid
4. Optimize with respect to AEP.

The reasoning behind the constraints, such as using a realistic boundary area and assuming the layout must be a grid, are that these are typical constraints of offshore wind farms, and we expect them to apply to the U.S. offshore locations for reasons such as shipping lanes. The selection of maximizing AEP as the objective of the layout optimization is an assumption that will be important in interpreting the results and will be discussed further.

The boundary areas for each location are taken from BOEM offshore wind lease areas or call areas and are illustrated in Figure 5. It should be noted that in the case of Humboldt, the boundary modeled is not the final selection but one from an earlier report before the final decision (Option B in Cooperman et al. [2022]). Note that for the sake of computational tractability, the areas were downscaled such that a typical layout optimization could fit approximately 50 wind turbines into the area. We believe this compromise, which enables many more optimizations to run, still maintains the essential features of a large array.

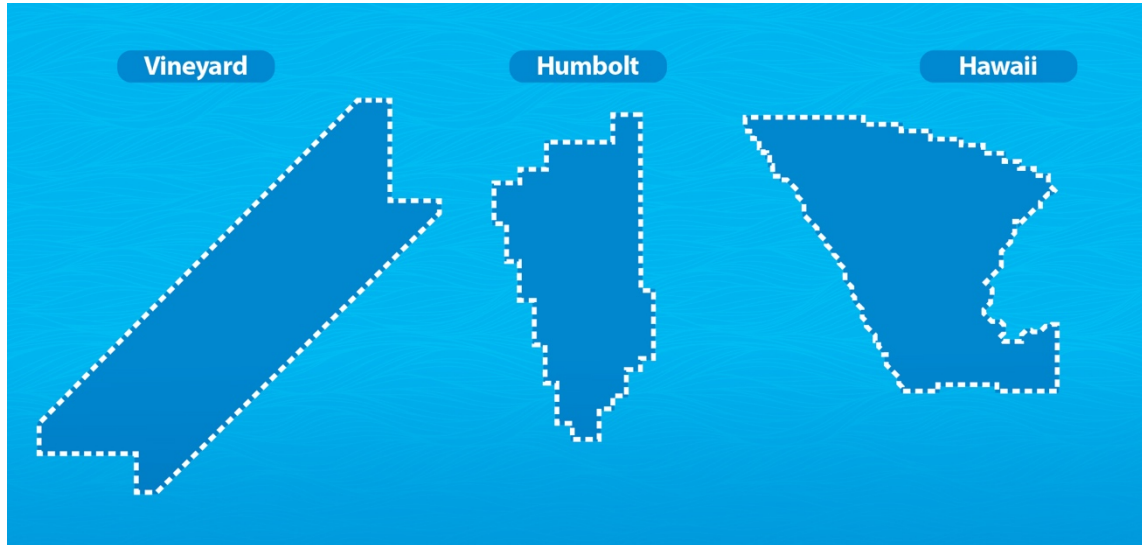


**Figure 5. Boundary areas for study of US offshore locations**

As mentioned earlier, the layout designs were optimizations over gridded layouts. To define a given grid, we adopted the terminology of Figure 6, with those terms defining a given grid. Bearing angle sets the rotation of the grid relative to the north-south alignment of the columns, whereas row shift offsets the turbines from row to row. Bearing and cross-bearing offset translate the grid along the axis set by the bearing angle. In this work, we assume a fixed interturbine distance (minimum distance and cross-bearing distance in the figure) of 1 nm as an externally provided constraint.

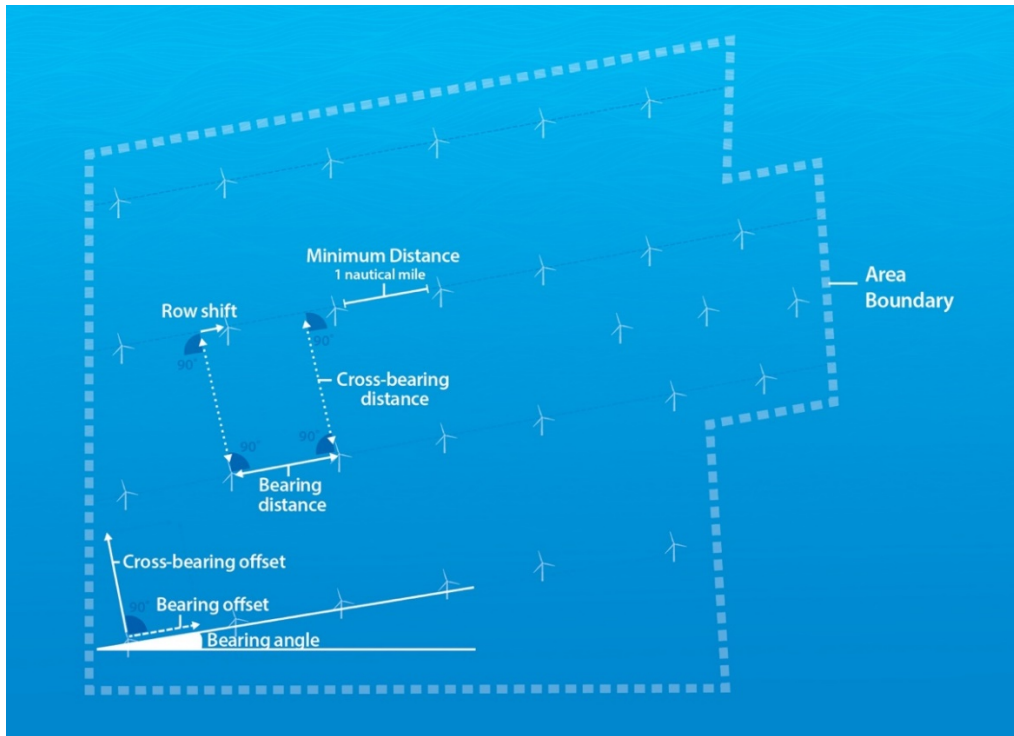


**Figure 6. Definition of terms that define a given grid layout. *Figure adapted from the original version courtesy of David Kyle and Jared Kassebaum of EDF Renewables***

In conducting layout optimizations, we assumed several possible grid configurations that further specify how wind turbines can be laid out within the boundary area. “NorthSouth” grids assume the columns of the grid must be north-south aligned (bearing angle is 0). In this optimization, the only terms to optimize over are the bearing offset and cross-bearing offset. Note that the number of turbines is not fixed in advance. In the “Bearing” optimization, we include bearing angle in the set of variables to optimize over. “Bearing+Shift” adds row shift to the set of variables to optimize over. The “BoundaryGrid” layout uses the same grid parameterization as “Bearing+Shift” but allows wind turbines to be placed on the wind farm boundary separate from the internal grid structure as long as the minimum interturbine distance is maintained. Finally, “HexPacked” places turbines using a hexagonal pattern, which yields the densest possible layout while maintaining 1 nm between all turbines. These optimization types are illustrated in Figure 7.

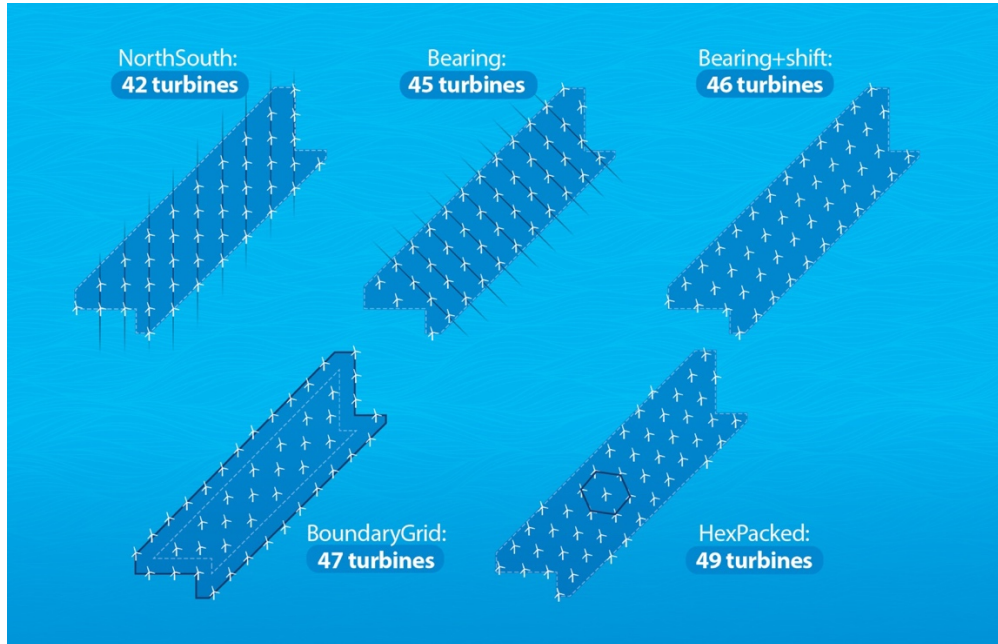


**Figure 7. The optimization layout methods considered. In each case, the AEP-optimal layout for Vineyard is shown.**

The wind turbine model used in the optimizations was a hypothetical 20-megawatt (MW) turbine based on the specifications provided in Sartori et al. (2018). The turbine has a rotor diameter of 252 m and a hub height of 165 m.

Finally, to test the stability of the optimization results for a number of model components, we ran a central setting as well as several alternative settings. For the wake model chosen within FLORIS, the central model was the CC model described earlier, and the alternative models were the GCH model and the TurbOPark model (OrstedRD 2022). The wind rose for each site was provided by the WRF analysis described in the central case and obtained from ERA-5 in the alternative. The interturbine spacing was fixed at 1 nm in the central case and shortened to 0.8 nm in the alternative. The turbine was the 20-MW model in the central case, and the International Energy Agency (IEA) 15-MW reference wind turbine in the alternative (Bortolotti et al. 2019). Finally, the TI was the 6% value found to fit the data best in the SCADA analysis, whereas the alternative TI was a lower 3% value. These central and alternative settings are summarized in Table 1.

**Table 1. Parameters for Central and Alternative Optimizations**

Parameter	Central Setting	Alternative Settings
Wake Model	CC	GCH, TurbOPark
Spacing	1 nautical mile	0.8 nautical miles
Wind Resource Provider	WRF (Task 1)	Era-5 / Merra-2
Turbine Model	X_20MW	IEA 15 MW
Turbulence Intensity	6%	3%

The results of the layout optimizations, with respect to AEP, wake losses, and number of turbines, for the central parameters are shown for each site in Figure 8. For all the alternative settings, the Task 3 report has more detail, but, in every case, only the absolute levels of the results change; the relative pattern is consistent across all parameterizations. In each pane, the wake losses, AEP (normalized to the NorthSouth case), and number of wind turbines are indicated. The results show that as the layout optimization becomes progressively less constrained, the layouts yield increasingly higher levels of AEP, which is the optimization objective. However, this is primarily achieved by accommodating higher numbers of turbines into the fixed boundary area; in many cases, the wake losses can actually increase with the increase in AEP. We infer from these results that layout optimization, when AEP is the objective, can first be seen as maximizing the number of turbines allowed in the area under a given set of constraints, and second as minimizing wake losses. Note that while somewhat more complex, this tendency to maximize number of turbines first and wake losses second is observed in locations with directionally concentrated wind roses (Humboldt and Hawaii).

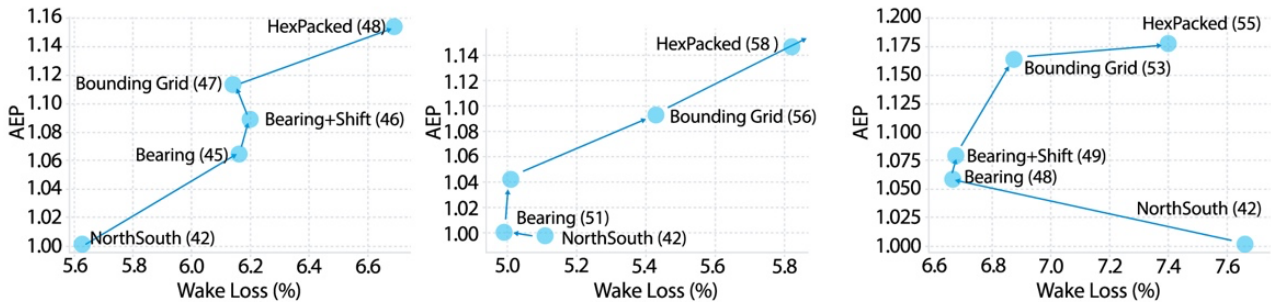


**Figure 8. Layout optimization results for each site and optimization case for the central parameterization for Vineyard (left), Humboldt (middle), and Hawaii (right).**

### 3.2 Wind Farm Control Optimization

The results of the layout optimizations could then be used as inputs to wind farm control optimization. For each site and optimized layout (and for each parameterization of the central and alternative parameter settings), an optimization can be performed over turbine yaw control strategies to determine a wind farm

controller. Then, for each case, we can compare the AEP of the baseline case (without yaw control) to the AEP produced with wind farm control and calculate a percent gain in AEP. The results for all cases are shown in Figure 9.

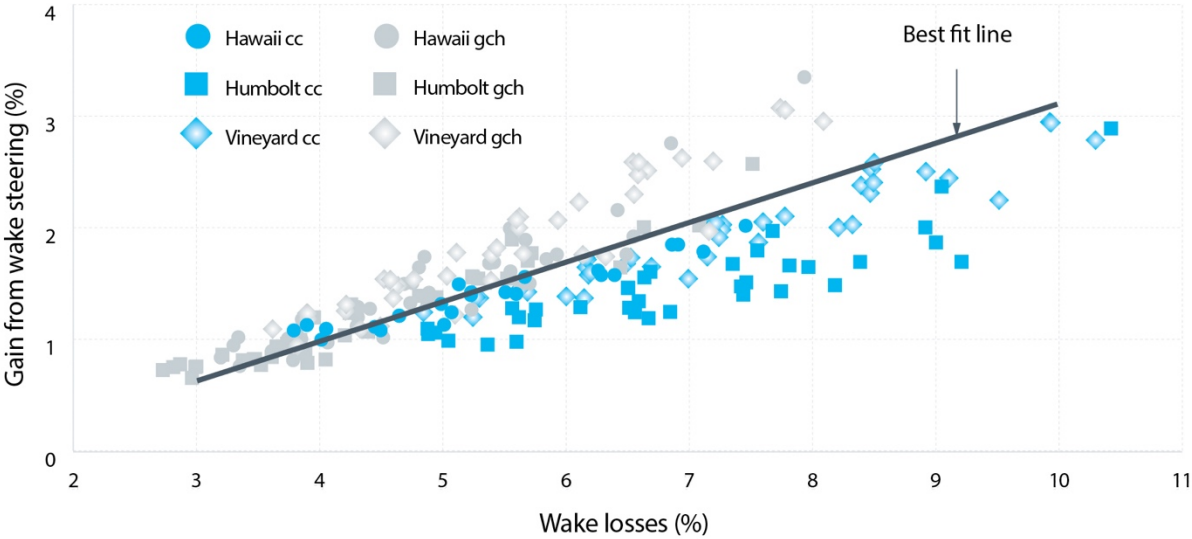


**Figure 9. Gain from wake steering for every case versus initial wake losses. The trend is linear; however, compared to SOWFA simulations, we observed that GCH tended to slightly overpredict gains, whereas CC tended to underpredict. Therefore, an approach of fitting to both resulted in a useful compromise.**

Figure 9 presents the gain in AEP from yaw control for every case against the wake losses in the baseline case. The results show that the gain in AEP from yaw control correlates well to underlying wake losses. As described earlier, in comparison with large-eddy simulation results, the GCH model had some tendency to overpredict gains for large arrays, whereas the CC model tended to underpredict (the models are similar for small numbers of turbines). Therefore, for the purpose of this project, we determined a reasonable approach to be a best-fit line to this full set of data points, all parameterizations, for both the CC and GCH models, effectively splitting the difference. Note that TurbOPark is not included in this fitting, as its wake-steering component was not calibrated in FLORIS in the earlier work. The linear fit yields an equation to estimate wake-steering uplift given wake losses:

$$\text{Percent gain from yaw control} = (\text{wake losses} \times 0.35) - 0.4$$

Using this equation allows us to calculate the expected gains from wake steering in each of the central cases. Calculating this uplift for each layout optimization in the central parameter set gives the results shown in Figure 10.

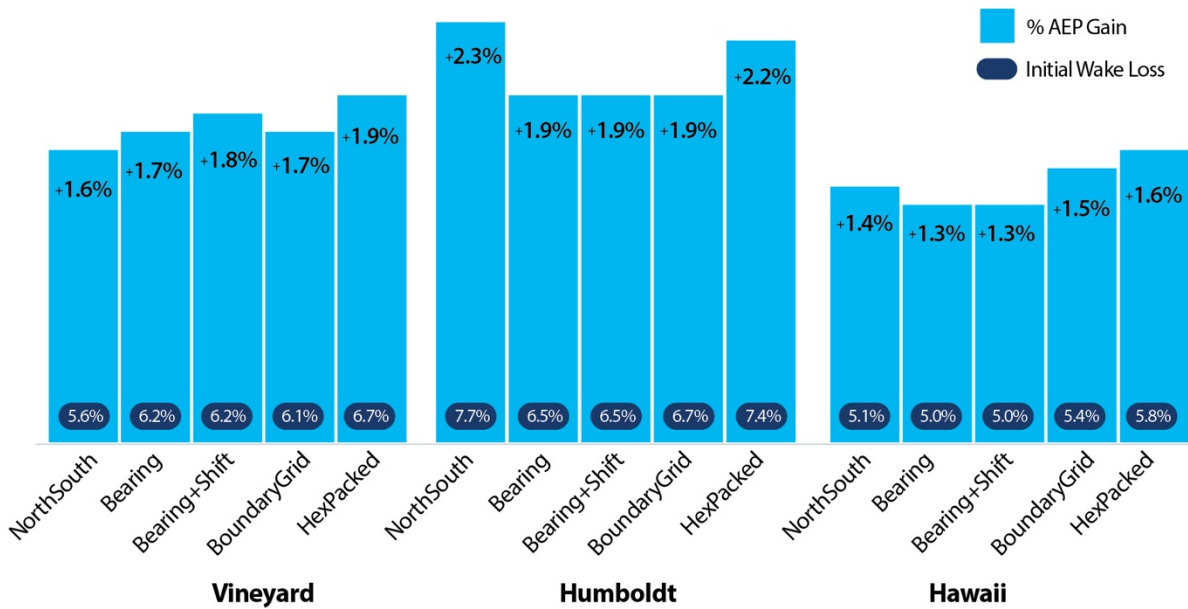


**Figure 10. Gains from wake steering (in steady state) for each location and layout optimization. Initial wake losses are indicated in each case.**

### 3.2.1 Considerations on Wind Farm Control Results

It is important to point out that these gains from AEP are steady-state results. Achievable gains are limited in practice by dynamic considerations, in which perfectly tracking an offset is not possible. Kanev (2020) proposes that a well-designed wake-steering controller might yield up to 80% of the underlying static benefits as expressed in this report. Other potential sources of reduction in gain from the steady-state result would be limitations on when wake steering can be applied, and limitations of total offset amounts, driven by turbine load considerations (e.g., because of limits on yawing or partial waking). Another important caveat is that these results do not consider that these farms have been modeled without including neighboring wind farms, which can further impact results.

### 3.3 Discussion of Optimization Results

The results of both layout optimization and wind farm control optimizations for each site and layout type are provided in Table 2.

**Table 2. Final Results of Optimization Analysis**

Site	Layout option	Baseline AEP	Wake loss %	Number of turbines	Wake steering AEP	% AEP Gain
Vineyard	NorthSouth	3730.0	5.6%	42	3788.3	+1.6%
	Bearing	3973.7	6.2%	45	4043.2	+1.7%
	Bearing+Shift	4060.6	6.2%	46	4132.0	+1.8%
	BoundaryGrid	4151.1	6.1%	47	4223.4	+1.7%
	HexPacked	4302.5	6.7%	49	4385.6	+1.9%
Humboldt	NorthSouth	3669.8	7.7%	46	3753.2	+2.3%
	Bearing	3878.0	6.5%	48	3950.3	+1.9%
	Bearing+Shift	3958.4	6.5%	49	4032.4	+1.9%
	BoundaryGrid	4274.3	6.7%	53	4356.5	+1.9%
	HexPacked	4401.1	7.4%	55	4496.8	+2.2%
Hawaii	NorthSouth	4578.0	5.1%	51	4641.7	+1.4%
	Bearing	4584.9	5.0%	51	4646.4	+1.3%
	Bearing+Shift	4763.5	5.0%	53	4827.8	+1.3%
	BoundaryGrid	5010.8	5.4%	56	5085.7	+1.5%
	HexPacked	5257.5	5.8%	59	5343.2	+1.6%

The results of this section lead to some key points. In the case where the target of optimization is AEP and the constraints are limited to interturbine spacing and lease area boundary, we find that layout optimization will effectively produce a layout that maximizes the number of wind turbines and, within the set of maximum number turbine layouts, minimizes wake losses. Because layout optimization as defined in this work only minimizes wake losses as a secondary consideration, it can leave ample room for wind farm control strategies to provide a valuable increase in AEP by reducing the remaining wake losses. A surprising outcome of this is that the Humboldt site, with highly directionally concentrated winds, is consistently the highest-value location for wake steering because, again, the layout optimization trades off not reducing wake losses in favor of increasing the number of wind turbines.

Much of this result is a consequence of optimizing for AEP and not LCOE, which would have applied a counterweight to the tendency to add more turbines by including the cost to those turbines. However, the AEP objective was selected with the project advisory board as being consistent with expected practices, wherein given limited lease areas, developers will try to maximize the energy production capacity. Recent events that occurred after this analysis was conducted seem to support this assumption. For example, Buljan (2022) includes announcements by the following winning bidders in the California offshore wind energy auction (which includes the Humboldt area):

“Equinor, RWE, Ocean Winds, and CIP have announced immediately after being revealed as provisional winners that their lease areas have the potential to host around 2 GW (Equinor), 2 GW (Ocean Winds), 1.6 GW (RWE), and over 1 GW (Copenhagen Infrastructure Partners) of installed capacity. Shortly after

this, Invenergy also said via social media that its lease area has an installation capacity of 1.5+ GW. This is well beyond the originally estimated lease area capacities and almost double the expected total capacity of 4.5 GW, which now climbed to at least 8.1 GW” (Buljan 2022).

This near-doubling of expected total capacity is consistent with a layout optimized toward maximum AEP given a constrained boundary area. In general, the results from this project indicate that wake steering can be a valuable asset in U.S. offshore wind energy production in the event that constrained layouts and the need to maximize total capacity yield wind farms not optimized to minimize wake losses, since the value of wake steering is shown to increase as wake losses increase.

Since the computational burden of simulating very large arrays with wake control is beyond current resources, it is worth noting that most of the developed wind farms will likely contain several hundred wind turbines where deep array wake losses will be experienced away from the wind farm edges. As shown above, accurately modeling wake steering for large arrays is a subject of active research. This might meaningfully impact the results of wake steering in a different way than for the wind farms of around 50 wind turbines studied here, which typically have around four “rows” or “columns” for wakes to develop and merge laterally and downwind. Furthermore, lease areas like Vineyard will not experience freestream winds from all directions but will be subject to both near wakes from turbines in adjoining lease areas and potentially far wakes from wind farms not adjoining but within distances of up to 90 km. These impacts require further study.

## 4. LCOE and Revenue Analysis

In the final project phase, the LCOE for each of the layout optimizations in Table 2 were derived with and without the effect of wind farm control on AEP. The results are shown in Figure 11.

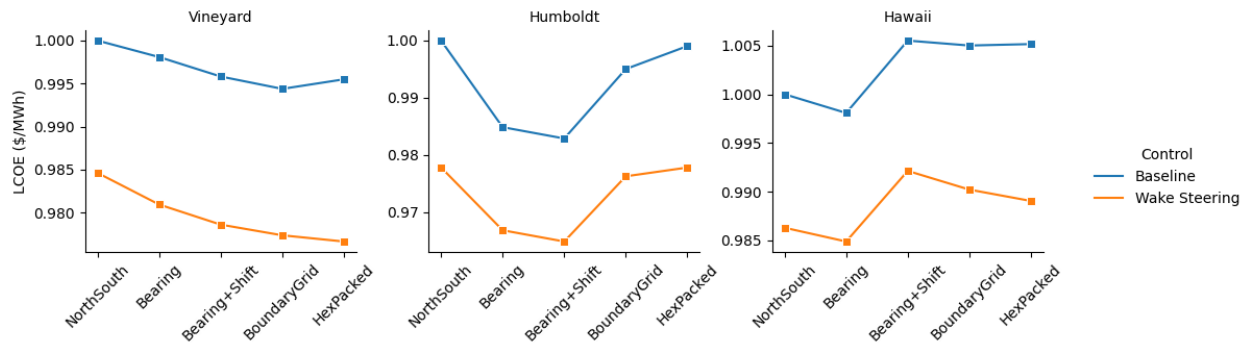


**Figure 11. LCOE for each site and layout optimization with and without wind farm control, normalized to the NorthSouth baseline (not wake steering) case.**

The methods used in computing the LCOE are fully detailed in the Task 4 report. For each location, we derived a proposed cable layout manually, and then the LCOE could be derived using NREL’s Offshore Renewables Balance-of-System and Installation Tool (ORBIT) (Nunemaker et al. 2020). Operations and maintenance costs were assumed to be in line with the median survey response from Wiser et al. (2021). With respect to LCOE, the layout optimizations are not ordered in the same way as AEP; however, this is expected given the costs of additional wind turbines. Note that the AEP uplift from wake steering produces a linear reduction in LCOE.

### 4.1 Revenue Analysis

In a journal article that is currently under review, we explored the expected impact of wind farm control on wind farm revenue, in addition to the usually calculated AEP, for land-based wind energy farms across the continental United States. The results showed the impact on revenue in every case exceeded those of AEP impact, in large part because the electricity prices in below-rated wind speeds (where wake steering can be applied) exceeded those in above-rated wind speeds (where wake steering can have no impact because wake losses go to zero at these speeds).

A small study was added to this project to assess possible impacts to revenue for offshore wind farms from wind farm control. The results of this study are shown in Figure 12.

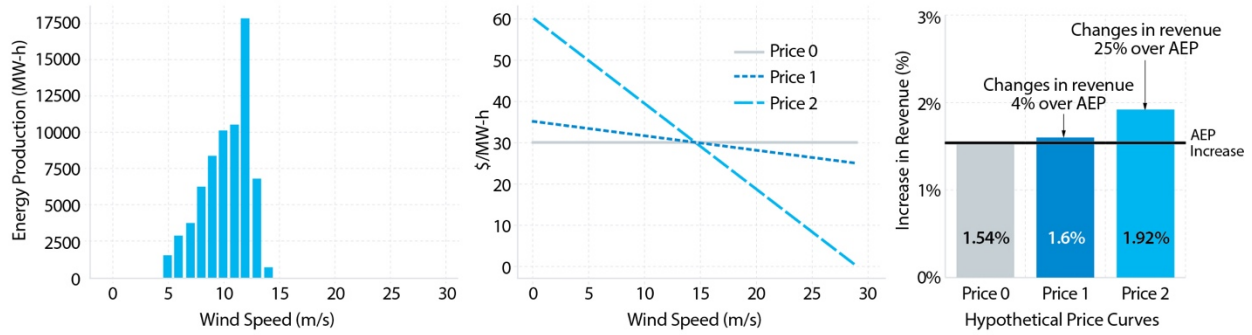


**Figure 12. (Left) Distribution of extra energy production from wake steering binned by wind speed for Vineyard. (Middle) Three hypothetical simple relationships between mean wind speed and energy prices. (Right) Combining the AEP results and hypothetical price curves shows how as the price curve steepens (such that higher wind speeds are associated with lower energy prices), the amount by which revenue gains exceed AEP gains increases.**

In Figure 12, increases in energy production for one of the Vineyard layouts is shown, binned by wind speed. Note that all gains come from wind speeds just above the rated wind speed of the turbines (11.4 m/s) and below. In the middle plot, we show three simplistic linear relationships between wind speeds and electricity market prices that could develop as the amount of offshore wind farms in an area increases. The energy results and theoretical price curves are then used to compute estimated gains in energy and revenue. These are shown in the right subplot. The revenue gain exceeds the AEP gain as the slope of the hypothetical prices becomes increasingly steep. This relationship is another way in which wind farm control could potentially add value to U.S. offshore wind farms, by increasing energy production during times of higher electricity value.

## **5. Conclusions**

---

This report reviewed the results and main conclusions of the project “Wind Farm Control and Layout Optimization for U.S. Offshore Wind Farms.” A key finding is that wake steering should be considered a valuable tool for increasing the energy production of wind farms, especially in the event the farms are designed to maximize the energy production of a given boundary area. As the U.S. offshore wind energy industry grows, the value of wake steering with respect to wind farm revenue is expected to exceed that of AEP alone.

## References

---

- Atmosphere to Electrons. 2023. “Lidar – California – Leosphere Windcube 866 (120), Humboldt – Processed Data.” U.S. Department of Energy. <https://a2e.energy.gov/data/buoy/lidar.z05.a0>.
- Bastankhah, M., B. L. Welch, L. A. Martinez-Tossas, J. King, and P. Fleming. 2021. “Analytical Solution for the Cumulative Wake of Wind Turbines in Wind Farms.” *Journal of Fluid Mechanics* 911 <https://doi.org/10.1017/jfm.2020.1037>.
- Bay, C. J., P. Fleming, B. Doekemeijer, J. King, M. Churchfield, and R. Mudafort. 2022. “Addressing Deep Array Effects and Impacts to Wake Steering With the Cumulative-Curl Wake Model.” *Wind Energy Science Discussions* [preprint] <https://doi.org/10.5194/wes-2022-17>.
- Bensason, D., E. Simley, O. Roberts, P. Fleming, M. Debnath, J. King, C. Bay, and R. Mudafort. 2021. “Evaluation of the Potential for Wake Steering for U.S. Land-Based Wind Power Plants.” *Journal of Renewable and Sustainable Energy* 13(3): 033303. <https://doi.org/10.1063/5.0039325>.
- Blondel, F., and M. Cathelain. 2020. “An Alternative Form of the Super-Gaussian Wind Turbine Wake Model.” *Wind Energy Science* 5(3): 1225–1236. <https://doi.org/10.5194/wes-5-1225-2020>.
- Bodini, N., J. K. Lundquist, and A. Kirincich. 2019. “U.S. East Coast Lidar Measurements Show Offshore Wind Turbines Will Encounter Very Low Atmospheric Turbulence.” *Geophysical Research Letters* 46(10): 5582–5591. <https://doi.org/10.1029/2019GL082636>.
- Bortolotti, P., H. Canet Tarres, K. Dykes, K. Merz, L. Sethuraman, D. Verelst, and F. Zahle. 2019. *IEA Wind Task 37 on Systems Engineering in Wind Energy WP2.1 Reference Wind Turbines*. International Energy Agency. NREL/TP-5000-73492. <https://www.nrel.gov/docs/fy19osti/73492.pdf>.
- Buljan, A. 2022. “California Lease Sale Winners Are: RWE, Equinor, CIP, Ocean Winds, and Invenergy. Floating Wind Farm Capacities Higher Than Initially Estimated.” OffshoreWIND.biz. <https://www.offshorewind.biz/2022/12/07/california-lease-sale-winners-are-rwe-equinor-cip-ocean-winds-and-inenergy-floating-wind-farm-capacities-higher-than-initially-estimated/>.
- Bureau of Ocean Energy Management (BOEM). Undated[a]. “Vineyard Wind 1.” <https://www.boem.gov/vineyard-wind>.
- Bureau of Ocean Energy Management (BOEM). Undated[b]. “California Activities.” <https://www.boem.gov/renewable-energy/state-activities/california>.
- Bureau of Ocean Energy Management (BOEM). Undated[c]. “Hawai’i Activities.” <https://www.boem.gov/renewable-energy/state-activities/hawaii-activities>.
- Cooperman, A., P. Duffy, M. Hall, E. Lozon, M. Shields, and W. Musial. 2022. *Assessment of Offshore Wind Energy Leasing Areas for Humboldt and Morro Bay Wind Energy Areas, California*. Golden, CO: National Renewable Energy Laboratory. NREL/TP-5000-82341. <https://www.nrel.gov/docs/fy22osti/82341.pdf>.

- Doekemeijer, B. M., E. Simley, and P. Fleming. 2022. “Comparison of the Gaussian Wind Farm Model With Historical Data of Three Offshore Wind Farms.” *Energies* 15(6): 1964. <https://doi.org/10.3390/en15061964>.
- Fleming, P., J. King, E. Simley, J. Roadman, A. Scholbrock, P. Murphy, J. K. Lundquist, et al. 2020. “Continued Results From a Field Campaign of Wake Steering Applied at a Commercial Wind Farm – Part 2.” *Wind Energy Science* 5(3): 945–958. <https://doi.org/10.5194/wes-5-945-2020>.
- Hahmann, A. N., T. Sīle, B. Witha, N. N. Davis, M. Dörenkämper, Y. Ezber, E. García-Bustamante, et al. 2020. “The Making of the New European Wind Atlas – Part 1: Model Sensitivity.” *Geoscientific Model Development* 13(10): 5053–5078. <https://doi.org/10.5194/gmd-13-5053-2020>.
- Kanev, S. 2020. “Dynamic Wake Steering and Its Impact on Wind Farm Power Production and Yaw Actuator Duty.” *Renewable Energy* 146: 9–15. <https://doi.org/10.1016/j.renene.2019.06.122>.
- King, J., P. Fleming, R. King, L. A. Martínez-Tossas, C. J. Bay, R. Mudafort, and E. Simley. 2021. “Control-Oriented Model for Secondary Effects of Wake Steering.” *Wind Energy Science* 6(3) 701–714. <https://doi.org/10.5194/wes-6-701-2021>.
- Musial, W., P. Spitsen, P. Duffy, P. Beiter, M. Marquis, R. Hammond, and M. Shields. 2022. *Offshore Wind Market Report: 2022 Edition*. Washington, D.C.: U.S. Department of Energy. DOE/GO-102022-5765. <https://www.energy.gov/sites/default/files/2022-09/offshore-wind-market-report-2022-v2.pdf>.
- National Renewable Energy Laboratory. 2022. “NREL/floris.” GitHub. <https://github.com/NREL/floris>.
- National Renewable Energy Laboratory. 2021. “Offshore Wind Data Release Propels Wind Prospecting.” <https://www.nrel.gov/news/program/2021/offshore-wind-data-release-propels-wind-prospecting.html>.
- National Renewable Energy Laboratory. Undated. “SOWFA: Simulator fOr Wind Farm Applications.” <https://www.nrel.gov/wind/nwtc/sowfa.html>.
- NCAR. 2023. “Weather Research & Forecasting Model (WRF).” <https://www.mmm.ucar.edu/weather-research-and-forecasting-model>.
- Nunemaker, J., M. Shields, R. Hammond, and P. Duffy. 2020. *ORBIT: Offshore Renewables Balance-of-System and Installation Tool*. Golden, CO: National Renewable Energy Laboratory. NREL/TP-5000-77081. <https://www.nrel.gov/docs/fy20osti/77081.pdf>.
- OrstedRD. 2022. “OrstedRD/TurbOPark.” GitHub. <https://github.com/OrstedRD/TurbOPark>.
- Pryor, S. C., R. J. Barthelmie, and T. C. Shepherd. 2021. “Wind Power Production From Very Large Offshore Wind Farms.” *Joule* 5(10) 2663–2686. <https://doi.org/10.1016/j.joule.2021.09.002>.
- Rosencrans, D., J. Lundquist, M. Optis, A. Rybchuk, N. Bodini, and M. Rossol. In review. “Annual Variability of Wake Impacts on Mid-Atlantic Offshore Wind Plant Deployments.” *Nature Energy*.
- Sartori, L., F. Bellini, A. Croce, and C. L. Bottasso. 2018. “Preliminary Design and Optimization of a 20MW Reference Wind Turbine.” *Journal of Physics: Conference Series* 1037: 042003. DOI 10.1088/1742-6596/1037/4/042003.

Simley, E., P. Fleming, N. Girard, L. Alloin, E. Godefroy, and T. Duc. 2021. “Results From a Wake-Steering Experiment at a Commercial Wind Plant: Investigating the Wind Speed Dependence of Wake-Steering Performance.” *Wind Energy Science* 6(6): 1427–1453. <https://doi.org/10.5194/wes-6-1427-2021>.

Slater, N. J. 2021. “DNV and Partners Begin UK-US Research Project To Investigate the Application of Wake Steering on Floating Offshore Wind Farms.” DNV.com. <https://www.dnv.com/news/dnv-and-partners-begin-uk-us-research-project-to-investigate-the-application-of-wake-steering-on-floating-offshore-wind-farms-203917>.

The White House. 2021. “FACT SHEET: Biden Administration Jumpstarts Offshore Wind Energy Projects To Create Jobs.” <https://www.whitehouse.gov/briefing-room/statements-releases/2021/03/29/fact-sheet-biden-administration-jumpstarts-offshore-wind-energy-projects-to-create-jobs/>.

Wagenaar, J. W., L. A. H. Machielse, and J. G. Schepers. 2012. “Controlling Wind in ECN’s Scaled Wind Farm.” Presented at the EWEA 2012, Copenhagen, Denmark, April 16–19, 2012. ECN-M—12-007. <http://www.ecn.nl/docs/library/report/2012/m12007.pdf>.

Wiser, R., J. Rand, J. Seel, P. Beiter, E. Baker, E. Lantz, and P. Gilman. 2021. “Expert Elicitation Survey Predicts 37% to 49% Declines in Wind Energy Costs by 2050.” *Nature Energy* 6: 555–565. <https://doi.org/10.1038/s41560-021-00810-z>.